



Egyptian Journal of Physics

<https://ejphysics.journals.ekb.eg/>

Thermodynamic Parameters for Rotating Ultracold Atomic Fermi Gases



Ahmed S. Hassan , Alyaa A. Mahmoud and Ebtsam A. Eid*

Physics Department, Faculty of Science, Minia University, El Minia, Egypt.

Abstract

In this paper, the thermodynamic parameters of a rotating ultracold atomic Fermi gas has been theoretically investigated. The analysis was based on a semiclassical approximation which is Sommerfeld expansion for the integral over the energy. Based on this result, several thermodynamic quantities are subsequently derived, such as the grand canonical thermodynamic potential, total energy, heat capacity and entropy. We subsequently explored how the rotation rate and interaction parameters influence various thermodynamic properties of the system. The results clearly indicate that these thermodynamic quantities are influenced by the rotation rate , while at the same time, they remain unaffected by the trap parameters across all temperature ranges. By using specific heat as an indicator, we also examined the phase transition from the gas phase to the degenerate phase. The methodology presented here can be extended to investigate the thermodynamic properties of a rotating Bose gas subjected to a combined harmonic and lattice potential.

Keywords: thermodynamic parameters, rotating ultracold atomic Fermi gas, semiclassical approximation, rotation rate, interaction parameters.

Introduction

Ultracold atomic Fermi gases offer numerous significant advantages that significantly improve our comprehension of the many-body physics of fermions. Due to their distinct characteristics and emerging occurrences, quantum many-body phases are a subject of ongoing investigation. Theoretical and experimental communities have been interested in ultracold molecular Fermi gases for several years [1–4]. The main objectives of these endeavors are to model new states of matter, including supersolids and nonconventional superfluid. In addition to studying, the Fermi-Hubbard model experimentally in a pure, isolated environment with full control over all Hubbard parameters [5,6] liquid ^3He [7], high temperature superconductors [8], and neutron stars [9].

Consideration should be given to trapped degenerate Fermi gases as a potential model for coupled Fermi condensates at lower temperatures as well as as a degenerate quantum system. Despite the fact that the ideal Fermi gas is a well-understood problem, the non-interacting Fermi gas is a good zeroth-order approximation in many well known systems. The interactions between atoms in Fermi gases are primarily short-range and have weak effects in the dilute limit. In numerous instances, interactions can be disregarded or viewed as a minor disturbance, such as in spin-polarized gases where the Pauli exclusion principle significantly reduces interactions at low temperature [10–12].

The temperature at which phase transition from normal gas to degenerate gas, dependence on various factors. Including the density of the gas, and the external trapping potential. In general, the transition temperature is determined by the balance between the thermal energy of the atoms and the attractive interactions that drive them to form a degenerate state. To understand the temperature properties of degenerate fermion, it is helpful to consider the concept of quantum statistics. Fermionic atoms obey the Pauli exclusion principle. This principle leads to the formation of a degenerate Fermi gas at low temperatures, where the fermions occupy the lowest available energy states, forming a Fermi sea. In many cases the role of interactions can in fact be neglected, as in the case of spin polarized gases where interactions are strongly suppressed at low temperature by the Pauli exclusion principle or treated as a small perturbation.

*Corresponding author: Ebtsam A. Eid, E-mail: *ebtsamali@mu.edu.eg.

Received: 19 July 2025; Accepted: 05 August 2025

DOI: 10.21608/ejphysics.2025.405623.1114

©2025 National Information and Documentation Center (NIDOC)

Basic formalism

Imagine a Fermi gas that is harmonically confined and has two spin states that are equally inhabited, as defined by the grand canonical ensemble. This gas is set up to rotate at an angular frequency of Ω around the z axis. The Hamiltonian of the particle in the spinning frame is provided by [13-15].

$$H = \frac{p^2 + p_z^2}{2M} + \frac{1}{2}M[\omega_\perp^2(x^2 + y^2) + \omega_z^2 z^2] - \Omega L_z$$

$$= \frac{|p_\perp - M\Omega \times r_\perp|^2}{2M} + \frac{p_z^2}{2M} + V_{rot}(r_\perp, z) \quad (1)$$

where

$$V_{rot}(r_\perp, z) = \frac{1}{2}M[\omega_\perp^2(1 - \alpha^2)r_\perp^2 + \omega_z^2 z^2] \quad (2)$$

where M is the atom mass, $r_\perp^2 = x^2 + y^2$, $\alpha = \frac{\Omega}{\omega_\perp}$ is the rotation rate, and $\omega_\perp \equiv \omega_x \equiv \omega_y$, ω_z is the harmonic oscillator frequencies.

Hamiltonian in Eq.(1) has energy-eigenvalues given by [16,17],

$$E(n_+, n_-, n) = n_+ \hbar \omega_\perp (1 - \alpha) + n_- \hbar \omega_\perp (1 + \alpha) + n_z \hbar \omega_z + E_0 \quad (3)$$

Where $E_0 = \hbar \omega_\perp + \frac{1}{2} \hbar \omega_z$ is the ground state energy, n_+ , n_- and n_z are positive integers.

Based on the partial derivative of the grand potential $\Omega(\alpha, T)$, which is the logarithm of the grand canonical partition function, all relevant parameters reflecting the superfluidity nature are obtained [18-20]. When all states are added up, the grand-canonical potential of an ideal Fermi gas can be expressed generally,

$$\Omega(\alpha, T) = \sum_{n_+, n_-, n_z=0} \ln(1 + e^{-\beta(E_{n_+, n_-, n_z} - \mu(T))}) \quad (4)$$

Where $\beta = (1/k_B T)$, and $\mu(T)$ is the chemical potential.

There is no analytically possible closed form evaluation for the sum in Eq. (4). An alternative method for performing this analysis would be to use an integral weighted by a suitable smooth density of states (DOS) $\rho(E)$, [21,22] to approximate the total i.e.

$$\Omega(\alpha, T) = \frac{1}{2} \int_0^\infty d\epsilon \rho(\epsilon) \ln[1 - n(\epsilon)] \quad (5)$$

with $\rho(\epsilon)$ is the density of states for non-interacting gas,

$$\rho(\epsilon) = \frac{1}{2} \frac{1}{(1 - \alpha^2)} \frac{\epsilon^2}{(\hbar \omega_g)^3} \quad (6)$$

where the geometrical average of the harmonic oscillator frequencies is $\omega_g = (\omega_\perp^2 \omega_z)^{1/3}$ and, $n(\epsilon) = \frac{1}{e^{\beta(\epsilon - \mu(T))} + 1}$ is the Fermi weighting factor. The chemical potential is fixed by the normalization condition [11]

$$N = \int_0^\infty d\epsilon \rho(\epsilon) n(\epsilon) \quad (7)$$

where N is required to be sufficiently large and being the number of atoms.

For later convenience, we should introduce a scaling behaviour of this many-body system. A first natural scaling parameter is given by the Fermi temperature T_F , the temperature characterizing the onset of quantum degeneracy phenomena. However, at $T = 0$ Eq.(7) allows one to calculate the Fermi energy, $E_F = \mu(T = 0, \alpha)$, defined as the energy at which all states below it are occupied and all states above it are unoccupied. The Fermi energy for nonrotating harmonic trap filled with N Fermions is given by,

$$E_F = k_B T_F = (6N)^{1/3} (\hbar \omega_g) \quad (8)$$

$$T_F = \frac{(6N)^{1/3}}{k_B} (\hbar \omega_g) \quad (9)$$

The temperature of a degenerate fermionic gas is typically measured in terms of the Fermi-temperature T_F . Below T_F , the ultra cold Fermion gas exhibits superfluid behavior, while above T_F , the system behaves as a normal gas. Consequently we should calculate the integral in Eq.(5) for these two limited.

For very low temperature, in the degenerate regime, substituting Eq.(6) into Eq.(5) and integrating by parts, one obtains the simplified integral

$$\Omega(\alpha, T) = \frac{\beta}{6} \int_0^\infty d\epsilon \frac{\epsilon \rho(\epsilon)}{e^{\beta(\epsilon - \mu(T))} + 1} \quad (10)$$

using Sommerfeld expansion,

$$\int_0^\infty \frac{\eta(\epsilon)}{e^{\beta(\epsilon - \mu(T))} + 1} d\epsilon = \int_0^{\mu(T)} \eta(\epsilon) d\epsilon + \sum_{n=1}^\infty a_n (k_B T)^{2n} \left. \frac{d^{2n-1} \eta(\epsilon)}{d\epsilon^{2n-1}} \right|_{\epsilon=\mu(T)} \quad (11)$$

with $\eta(\epsilon)$ being any function of ϵ , and

$$a_n = \left(2 - \frac{1}{2^{2(n-1)}} \right) \zeta(2n) \quad (12)$$

where $\zeta(n)$ is the Riemann zeta function. For $\eta(\epsilon) = \epsilon \rho(\epsilon)$, we have

$$\Omega(\alpha, T) = \frac{\beta}{6} \left[\int_0^{E_F} d\epsilon \epsilon \rho(\epsilon) + \int_{E_F}^{\mu(T)} d\epsilon \epsilon \rho(\epsilon) + a_1 (k_B T)^2 [\rho(\mu) + \mu \rho'(\mu)] \right. \\ \left. + a_2 (k_B T)^4 [3\rho''(\mu) + \mu \rho'''(\mu)] + a_3 (k_B T)^6 [4\rho'''(\mu) + \mu \rho''''(\mu)] \right] \quad (13)$$

The temperature dependence of $\mu(T)$ can be calculated using the Sommerfeld expansion, Eq.(11) [12]

$$\mu(T) = E_F - a_1 (k_B T)^2 \left. \frac{\rho'(\epsilon)}{\rho(\epsilon)} \right|_{\epsilon=E_F} = E_F \left[1 - a_1 \left(\frac{k_B T}{E_F} \right)^2 \right] \quad (14)$$

the other terms are vanished since the DOS is a quadratic function of energy.

In Eq.(13), the first integral is just, $\Omega_0(\alpha, 0) = 0$, the thermodynamic potential of the ground state at $T = 0$.

From Eq.(14) we know $|\mu(T) - E_F| \sim (k_B T)^2$ is small, we can approximate the second integral as,

$$\int_{E_F}^{\mu(T)} d\epsilon \epsilon \rho(\epsilon) \approx (\mu(T) - E_F) E_F \rho(E_F) = -a_1 (k_B T)^2 \left. \frac{\rho'(\epsilon)}{\rho(\epsilon)} \right|_{\epsilon=E_F} E_F \rho(E_F) \quad (15)$$

thus Eq.(13) gives

$$\Omega(\alpha, T) = \frac{\beta}{6} \left[-a_1 (k_B T)^2 \left. \frac{\rho'(E_F)}{\rho(E_F)} \right| E_F \rho(E_F) + a_1 (k_B T)^2 [\rho(\mu) + \mu \rho'(\mu)] + a_2 (k_B T)^4 [3\rho''(\mu) + \mu \rho'''(\mu)] \right. \\ \left. + a_3 (k_B T)^6 [4\rho'''(\mu) + \mu \rho''''(\mu)] \right] \quad (16)$$

Since $\mu(T) - E_F$ is small, we can evaluate the second term at $\mu(T) = E_F$ and finally have,

$$\Omega(\alpha, T) = \frac{1}{6} \left[a_1 (k_B T) \rho(\mu) + a_2 (k_B T)^3 [3\rho''(\mu) + \mu \rho'''(\mu)] + a_3 (k_B T)^5 [4\rho'''(\mu) + \mu \rho''''(\mu)] \right] \\ = \frac{1}{6} \frac{1}{(1 - \alpha^2)(\hbar \omega_g)^3} [a_1 (k_B T) \mu(T) + 3a_2 (k_B T)^3] \quad (17)$$

This is a general equation for the grand-canonical thermodynamic potential of a low-temperature ideal harmonically confined degenerate Fermi gas.

At high temperatures (classical limit $T \gg T_F$) Eq.(10) is approximated to,

$$\Omega_{>}(\alpha, T) = \frac{1}{6} \frac{\beta}{(1 - \alpha^2)(\hbar \omega_g)^3} \left[\int_0^{\mu(T)} d\epsilon \epsilon^3 e^{-\beta(\epsilon - \mu(T))} \right. \\ \left. + \int_{\mu(T)}^\infty d\epsilon \epsilon^3 e^{-\beta(\epsilon - \mu(T))} \right] \\ = \frac{1}{6} \frac{1}{(1 - \alpha^2)(\hbar \omega_g)^3} \left[\sum_{K=0}^3 \frac{3 \mu_{>}(T)^K}{\beta^{3-K}} \right] \quad (18)$$

the chemical potential, high temperature approximation for Eq.(7), is given by

$$\mu_{>}(T) = -k_B T \ln \left[\frac{6}{(1 - \alpha^2)} \left(\frac{k_B T}{E_F} \right)^3 \right] \quad (19)$$

Finally in terms of $\tau = \frac{T}{T_F}$, the thermodynamic potential is given by

$$\Omega_{\tau < 1}(\alpha, T) = \frac{N}{(1 - \alpha^2)} \left[\frac{\pi^2}{12} A^2 \tau + \frac{7\pi^4}{120} \tau^3 \right] \quad (20)$$

where $A = \left[1 - \frac{\pi^2}{3} \tau^2 \right]$, and

$$\Omega_{\tau > 1}(\alpha, T) = \frac{N \tau^3}{(1 - \alpha^2)} [\Omega_0(\alpha, 0) - B^3 + 3B^2 - 6B + 6] \quad (21)$$

where $B = \ln \left[\frac{6}{(1 - \alpha^2)} \tau^3 \right]$.

Here, we determine all for finite N from the state sum and compare it to the Sommerfeld approximation.

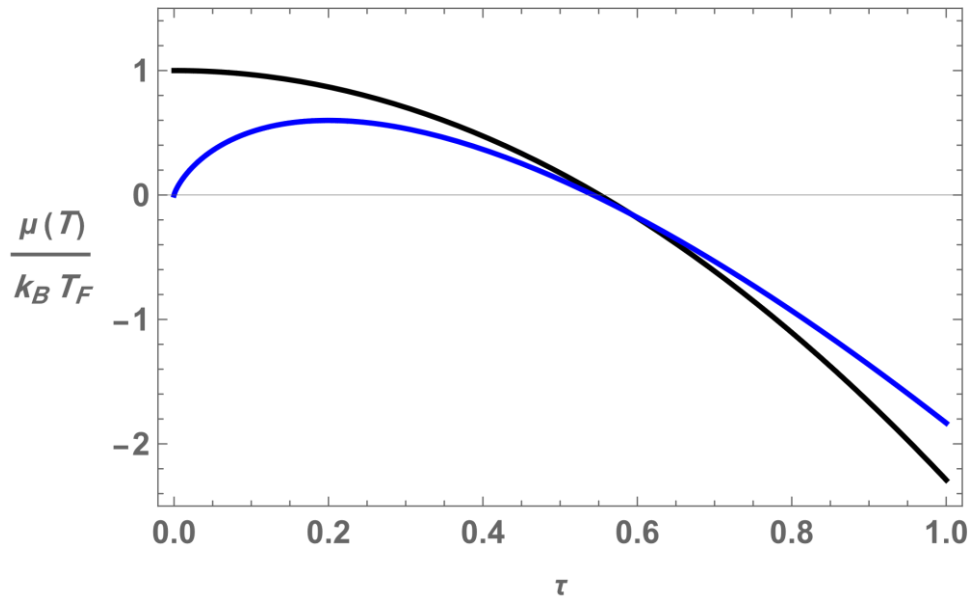


Fig.1. The chemical potential is plotted as a function of temperature, with both axes scaled by the Fermi temperature. This scaling produces a universal curve applicable to all harmonically trapped Fermi gases. Blue curve for $\tau > 1$ and dark for $\tau < 1$.

It is evident that the low temperature approximation remains quantitatively accurate below. $T/T_F \sim 0.6$.

Thermodynamic parameters

Total energy

Following the standard procedure, the total energy can be expressed in terms of the $\Omega(\alpha, T)$ -potential as follows

$$U = k_B T^2 \left(\frac{\partial \Omega(\alpha, T)}{\partial T} \right)_{\mu} \quad (22)$$

Substituting from Eqs.(20) and (21) in Eq.(22), the total energy per particle is given by,

$$\frac{U_{\tau < 1}}{N k_B T_F} = \frac{\pi^2 \tau^2}{12 (1 - \alpha^2)} \left[A^2 - \frac{4\pi^2 A \tau^2}{3} + \frac{21\pi^2 \tau^2}{10} \right] \quad (23)$$

for $\tau < 1$. While for $\tau > 1$ one has

$$\frac{U_{\tau > 1}}{N k_B T_F} = \frac{-3\tau^4}{(1 - \alpha^2)} [B^3] \quad (24)$$

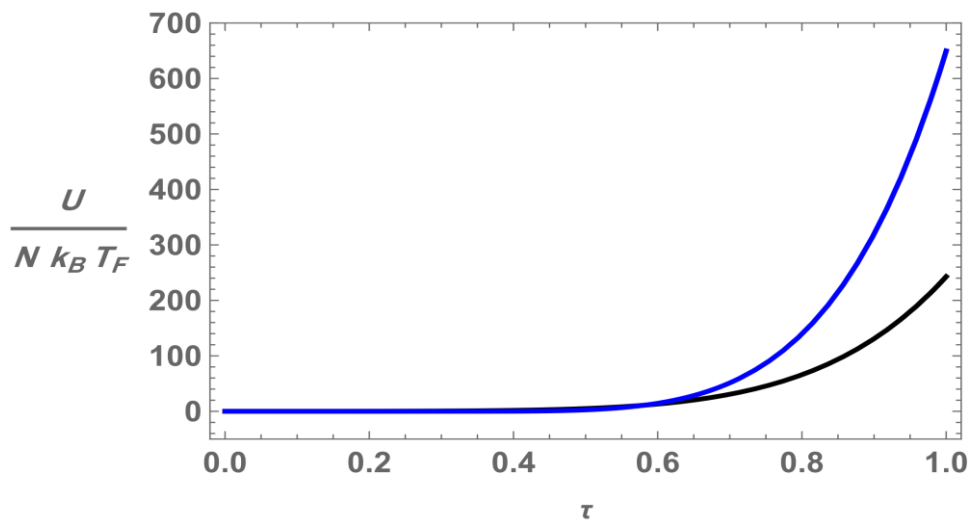


Fig.2. Total energy as a function of temperature. Blue curve for $\tau > 1$ and dark for $\tau < 1$.

Beginning with the energy, one can evaluate the specific heat, entropy, and other thermodynamic quantities.

Heat capacity

According to our approach, the specific heat can be written as

$$\frac{C_V(T)}{Nk_B} = \frac{\partial}{\partial T} (k_B T^2) \frac{\partial \Omega(\alpha, T)}{\partial T} \quad (25)$$

Substituting from Eq.(20) in Eq.(25), up to order (τ),

$$\Omega(\alpha, T) = \frac{N}{6} \left[\Omega_0(\alpha, 0) + \frac{\pi^2}{12} A^2 \tau \right] \quad (26)$$

The usual textbook Sommerfeld approximation for the specific heat at low temperatures, $\mu(T) = E_F$ i.e. in our approach $A = 1$, is recovered,

$$\frac{C_{V,\tau < 1}}{Nk_B} = \frac{\pi^2}{(1 - \alpha^2)} \frac{k_B T}{E_F} \quad (27)$$

For any value of $\mu(T)$ and $\tau < 1$, the heat capacity is given by,

$$\frac{C_{V,\tau < 1}}{Nk_B} = \frac{\pi^2}{6} \frac{1}{(1 - \alpha^2)} \left[A^2 \tau - \frac{10}{3} \pi^2 A \tau^3 + \frac{4}{9} \pi^4 \tau^5 + \frac{21}{5} \pi^2 \tau^3 \right] \quad (28)$$

While the heat capacity above $\tau > 1$ is given by

$$\frac{C_{V,\tau > 1}}{Nk_B} = - \frac{3\tau^3}{(1 - \alpha^2)} [4B^3 + 9B^2] \quad (29)$$

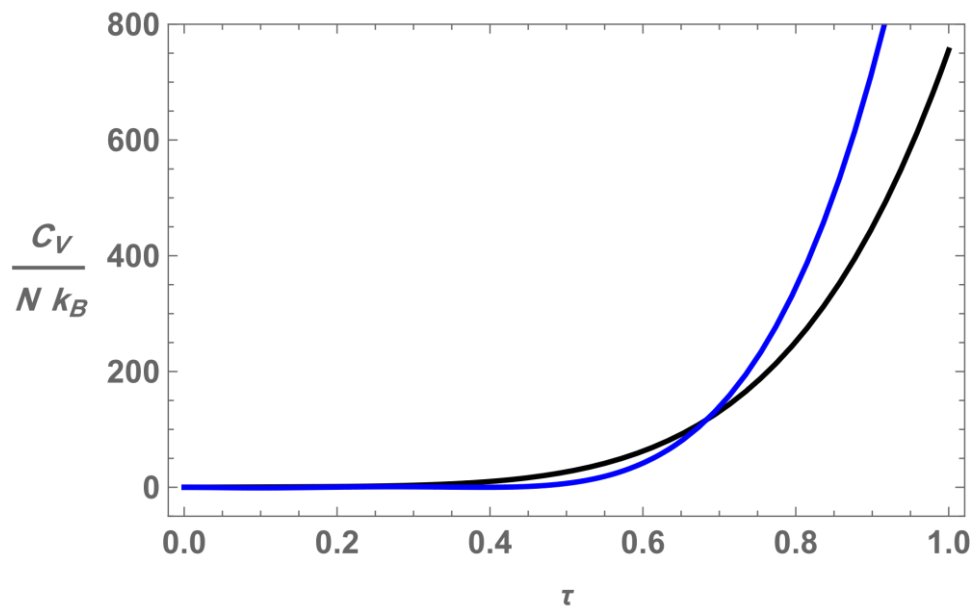


Fig.3. This plot shows the specific heat as a function of temperature. Blue curve for $\tau > 1$ and dark for $\tau < 1$.

The results obtained from Eqs. (28) and (29) are illustrated in Fig. 3 for various values of α . In this, we plot the normalized heat capacity C_V/Nk_B versus the normalized temperature τ , with the rotation rate α plays as a parameter. The heat capacity evolves, starting from zero, with increasing values proportional to the third power of the normalized temperature, that is: $C_V \propto \tau^3$. At $\tau = 1$ a steep jump takes place while it goes from $\tau < 1$ to $\tau > 1$. Above the critical temperature, a slow decrease with the temperature is observed in C_V . At high temperatures, the heat capacity approaches the temperature's independent behaviour expected for the non-interacting Bose gas: $3Nk_B$.

It is interesting to note that, signatures of a phase transition appear in the specific heat behaviour as a function of τ , α , and η . As T decreases, the phase transition, observed at $\tau = 1$, reveals the transition from non condensed state to those which is in condensed phase.

Entropy of the system

A primary objective in the study of degenerate Fermi gases is to reach very low temperatures which are accurate for condensed matter physics, such as quantum magnetism. However, to ascertain whether a given quantum phase is accessible, it is convenient to focus on its entropy, rather than temperature. Thus, it is important to determine and investigate the entropy-temperature curves[25]. The behaviour of these curves is used in analyzing the process of adiabatic cooling[25-27].

For the rotating condensate, the normalized entropy per particle is given by,

$$\frac{S}{N_\sigma k_B} = \frac{\Omega(\alpha, T)}{N_\sigma} + \frac{U}{N_\sigma k_B T} - \frac{\mu(T)}{k_B T} \quad (30)$$

Substituting from Eq's. (13), (14), (19), (24) and (23) in Eq. (30) we have,

$$\frac{S_{\tau < 1}}{N_\sigma k_B} = \frac{1}{(1 - \alpha^2)} \left[\frac{\pi^2}{6} A^2 \tau + \frac{7\pi^2}{120} \tau^3 - \frac{\pi^4}{9} A \tau^3 + \frac{7\pi^4}{40} \tau^3 - (1 - \alpha^2) \frac{A}{\tau} \right] \quad (31)$$

for $\tau < 1$, and

$$\frac{S_{\tau > 1}}{N_\sigma k_B} = \frac{\tau^3}{(1 - \alpha^2)} [-4B^3 + 3B^2 - 6B + 6] + B \quad (32)$$

for $\tau > 1$.

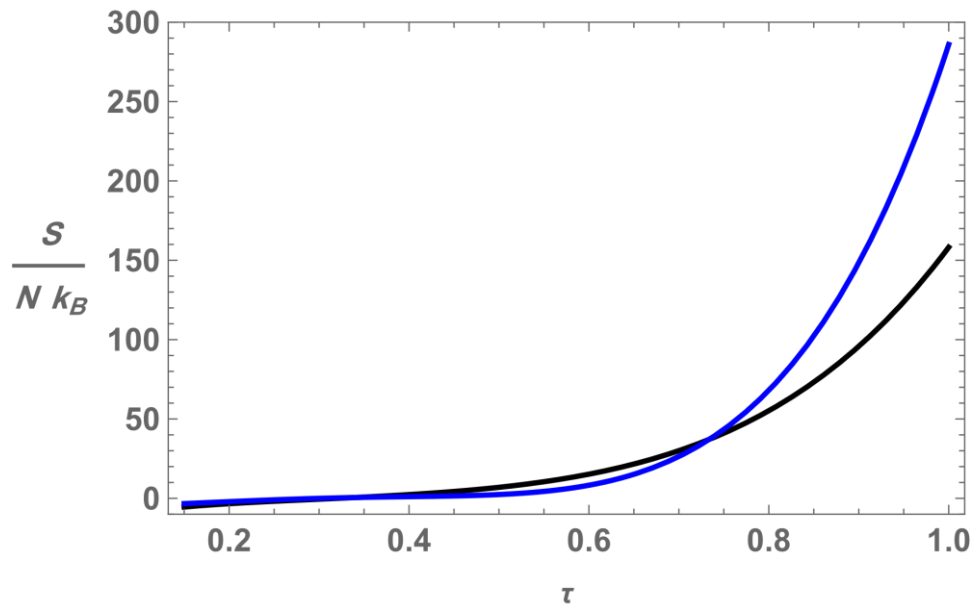


Fig.4. Plot of entropy versus temperature. The blue curve represents $\tau > 1$, and the dark curve represents $\tau < 1$.

In Fig.4 the entropy versus temperature curves, as a function of α and η , are given. These figures show that, as it is expected from standard thermodynamic arguments, that: as the temperature increases, the entropy has a monotonically increasing nature everywhere. Consequently, in order to achieve thermal equilibrium in rotating frame, the trap should contain an asymmetry in the xy -plane. Even very small asymmetries are sufficient to ensure thermal equilibrium and safe calculation of the relevant thermodynamic parameters. However, one of the sensitive quantities, to clear up the effects of the rotation and the interatomic interaction on the condensate, is the behavior of the heat capacity as a function of the reduced temperature.

Conclusion

In conclusion, by employing the Sommerfeld expansion approximation, we have derived analytical expressions for the thermodynamic potential and chemical potential of a rotating Fermi gas confined in an

axially symmetric harmonic potential. Subsequently, we obtained formulas for the total energy, specific heat, and entropy. Our results demonstrate that these thermodynamic quantities depend on the rotation rate while remaining independent of the trap parameters across the entire temperature range. Using the specific heat as an indicator, we also investigated the phase transition from the gas phase to the degenerate phase. The approach presented here can be extended to explore the thermodynamic properties of a rotating boson gas subjected to a combined harmonic and lattice potential.

Acknowledgments

Not available.

Funding statement

This study didn't receive any funding support

Declaration of Conflict of Interest

The authors declare that there is no conflict of interest.

References

- [1] Dimitrova, I., Flannigan, S., Lee, Y.K., Lin, H., Grilll, J.A., Jepsen, N., Cepait'e, I., Daley A. J. and Ketterle, W. (2023) Many-body spin rotation by adiabatic passage in spin-1/2 XXZ chains of ultracold atoms. *Quantum Science and Technology*, **8**, 035018. <https://doi.org/10.1088/2058-9565/acd2fb>
- [2] Mukherjee, B., Patel, P.B., Yan, Z., Fletcher, R.J., Struck, J. and Zwierlein, M.W. (2019) Spectral Response and Contact of the Unitary Fermi Gas. *Physical Review Letters*, **122**, 203402. <https://doi.org/10.1103/PhysRevLett.122.203402>
- [3] Eberz, D., Link, M., Kell, A., Breyer, M., Gao, K. and Ohl, M.K. (2023) Detecting the phase transition in a strongly interacting Fermi gas by unsupervised machine learning. *Phys. Rev. A*, **108**, 063303. <https://doi.org/10.1103/PhysRevA.108.063303>
- [4] Dom'inguez-Castro, G.A. and Paredes, R. (2020) Unconventional Superfluidity in Ultracold Dipolar Gases. *Journal of Physics: Conference Series*, **1540**, 012002. <https://doi.org/10.1088/1742-6596/1540/1/012002>
- [5] Hartke, T., Oreg, B., Jia, N. and Zwierlein, M. (2022) Quantum register of fermion pairs. *Nature*, **601**, 537. <https://doi.org/10.1038/s41586-021-04205-8>
- [6] Hartke, T., Oreg, B., Turnbaugh, C., Jia, N. and Zwierlein, M. (2023) Direct observation of nonlocal fermion pairing in an attractive Fermi-Hubbard gas. *Science*, **381**, 82. <https://doi.org/10.1126/science.ade4245>
- [7] Leggett, A.J. (1972) Interpretation of Recent Results on He3 below 3 mK: A New Liquid Phase. *Phys. Rev. Lett.*, **29**, 1227. <https://doi.org/10.1103/PhysRevLett.29.1227>
- [8] Lee, P.A., Nagaosa, N. and Wen, X. G. (2006) Doping a Mott insulator: Physics of high-temperature superconductivity. *Rev. Mod. Phys.*, **78**, 17. <https://doi.org/10.1103/RevModPhys.78.17>
- [9] Pethick, C. J. and Ravenhall, D. G. (1969) Matter at large neutron excess and the physics of neutron-star crusts. *Nature*, **224**, 673. <https://doi.org/10.1146/annurev.ns.45.120195.002241>
- [10] Carr, L. D., Shlyapnikov, G.V. and Castin, Y. (2004) Achieving a BCS Transition in an Atomic Fermi Gas. *Physical review letters*, **92**, 150404. <https://doi.org/10.1103/PhysRevLett.92.150404>
- [11] Giorgini, S., Pitaevskii, L.P. and Stringari, S. (2008) Theory of ultracold atomic Fermi gases. *Reviews of Modern Physics*, **80**, 1215. <https://doi.org/10.1103/RevModPhys.80.1215>
- [12] Butts, D.A. and Rokhsar, D.S. (1997) Trapped Fermi gases, *Phys. Rev. A*, **55**, 4346. <https://doi.org/10.1103/PhysRevA.55.4346>
- [13] Cooper, N.R. (2008) Rapidly Rotating Atomic Gases. *Advances in Physics*, **57**, 539. <https://doi.org/10.1080/00018730802564122>
- [14] Fletcher, R.J., Shaffer, A., Wilson, C.C., Patel, P.B., Yan, Z., Cr'epel, V., Mukherjee, B. and Zwierlein, M.W. (2021) Geometric squeezing into the lowest Landau level. *Science*, **372**, 1318. <https://doi.org/10.1126/science.aba7202>
- [15] Yong, S., Barbosa, S., Koch, J., Lang, F. and Pelster, A. (2023) Unravelling Interaction and Temperature Contributions in Unpolarized Trapped Fermionic Atoms in the BCS Regime. *cond-mat.quant-gas*, **2311.08853**. <https://doi.org/10.48550/arXiv.2311.08853>

- [16] Fetter, A.L. (2004) Vortices in rotating trapped dilute Bose–Einstein condensates. *Physica C*, **404**, 158. <https://doi.org/10.1016/j.physc.2003.09.104>
- [17] Hassan, A.S., El-Badry, A.M. and Soliman, S.S.M. (2011) Thermodynamic properties of a rotating Bose gas in harmonic trap. *Eur. Phys. J. D.*, **64**, 465–471 <https://doi.org/10.1140/epjd/e2011-20249-2>
- [18] Kirsten, K. and Toms, D.J. (1996) Bose-Einstein condensation of atomic gases in a general harmonic-oscillator confining potential trap. *Phys. Rev. A.*, **54**, 4188. <https://doi.org/10.1103/PhysRevA.54.4188>
- [19] Pathria, R.K. (1972) *Statistical Mechanics*, Pergamon, London. <http://linux0.unsl.edu.ar/~froma/MecanicaEstadistica/Bibliografia/PathriaBeale.pdf>
- [20] Blakie, P.B., Reyand, A.M. , Bezett, A. (2007) Thermodynamics of quantum degenerate gases in optical lattices. *Laser Physics*, **17**, 198. <https://doi.org/10.1134/S1054660X07020259>
- [21] Grossmann, S. and Holthaus, M. (1995) On Bose-Einstein condensation in harmonic traps. *Phys. Lett. A*, **208**, 188–192. [https://doi.org/10.1016/0375-9601\(95\)00766-V](https://doi.org/10.1016/0375-9601(95)00766-V)
- [22] Hassan, A.S. and El-Badry, A.M. (2014) Temperature dependence of the entropy and the in situ size of a rotating condensate cloud in an optical lattice. *Eur. Phys. J. D*, **68**, 76. <https://doi.org/10.1140/epjd/e2014-40571-3>
- [23] Blakie, P.B. , Bezett, A. and Buonsante, P.F. (2007) Degenerate Fermi gas in a combined harmonic-lattice potential. *Phys. Rev. A*, **75**, 063609. <https://doi.org/10.1103/PhysRevA.75.063609>
- [24] Catani, J., Barontini, G., Lamporesi, G., Rabatti, F., Thalhammer, G., Minardi, F., Stringari, S. and Inguscio, M. (2009) Entropy Exchange in a Mixture of Ultracold Atoms, *Phys. Lett. A*, **103**, 140401. <https://doi.org/10.1103/PhysRevLett.103.140401>
- [25] Olf, R., Fang, F., Marti, G.E., MacRae, A. and Stamper-Kurn, D.M. (2015) Thermometry and cooling of a Bose gas to 0.02 times the condensation temperature. *Nature Physics*, **11**, 720. <https://doi.org/10.1038/nphys3408>

المعاملات الديناميكية الحرارية للغازات الذرية الفيرمية فائقة البرودة الدوار

احمد سيد حسن، علياء عادل محمود و ابتسام على عيد

قسم الفيزياء، كلية العلوم، جامعة المنيا، مصر.

الملخص

في هذه الورقة البحثية، تم دراسة سلوك المعاملات الديناميكية الحرارية لغاز فيرمي الذري فائق البرودة دوار نظرياً. استند التحليل إلى تقريب شبه كلاسيكي، وهو توسع سومرفيلد، للتكامل على الطاقة. بناءً على هذه النتيجة، تم استخلاص العديد من الكميات الديناميكية الحرارية، مثل الجهد الديناميكي الحراري القياسي الكبير، والطاقة الكلية، والسعة الحرارية، والإنتروبيا. ثم استكشفنا كيف يؤثر معدل الدوران ومعاملات التفاعل على الخواص الديناميكية الحرارية. تشير النتائج إلى أن هذه الكميات الديناميكية الحرارية تتأثر بمعدل الدوران، لكنها تبقى غير متأثرة بمعاملات المصيدة عبر جميع نطاقات درجات الحرارة.

الكلمات الدالة: المعاملات الترموديناميكية، غاز فرمي ذري فائق البرودة دوار، التقريب شبه الكلاسيكي، معدل الدوران، معاملات التفاعل.